HETG

Dan Dewey, for the HETG Team

The HETG continues to perform as expected with no HETG-specific calibration changes made since the HETG efficiencies were updated in Dec 2011 (Marshall 2012). The main calibration change in the past year affecting the HETG was the update of the ACIS optical-blocking filter contamination model to version N0007 (in May 2012, included in CALDB 4.4.10 and later). This updated calibration applies mainly to observations made in/after 2010; the largest flux corrections (up to 25%) are below 1 keV.

A new data analysis tool for use with HETG data has been added to CIAO 4.5: `tg_findzo`, see the `ahelp` link in the references below. This tool determines the zeroth-order centroid with sub-pixel accuracy by making use of the readout-streak events; `tg_findzo` is particularly useful for bright sources where pileup may distort the zeroth-order image causing `tg_detect` to produce an inaccurate centroid.

In terms of modeling observed spectra, Beiersdorfer et al. (2012) show some impressive progress in combining atomic theory, laboratory measurement, and HETG astrophysical data. Their new calculations of the line wavelengths emitted by Fe XVI (Na-like Fe, i.e., having a single outer M-shell electron) very nicely explain residual emission seen in the very deep HETG Capella data that have been accumulated by *Chandra*, Fig. 1.

HETG Science: Motion at the Limits

The HETG's ability to measure Doppler velocities as low as 30 km s^{-1} has been put to good use over the course of the mission. Two examples from the past year involve orbital binary motion; both push the data to their statistical limits.

The system studied by Hussain et al. (2012) consists of two M-dwarfs of 0.6 M$_\odot$ each in a 0.81 day orbit and having velocities of about 120 km s^{-1}. Optical observations show eclipses and determine the orbital parameters. Two HETG observations that each lasted for a full orbit, ~ 70 ks, were made. The X-ray data show both flaring and quiescent emission. By extracting well-isolated emission lines and combining them in velocity space, they produce a composite line profile. This is done in a sliding time window to produce an image in velocity-time space (Figure 2). The identification of a flare to a specific binary component can be made based on the known component velocities and the observed velocity shift. The quiescent emission can likewise be studied by removing the flare times and by using only lines with low formation temperatures.

The mass ratio of objects in a binary can be determined if the orbital velocities of each component can be measured. For black holes it is hard to measure their orbital velocity, not only because they are black, but also because the emission from their accretion disks is dominated by continuum so that line measurements are generally not feasible. However Zhang et al. (2012) point out that accretion-disk winds can produce visible absorption lines in the spectrum and that these lines (with many caveats) should have the black
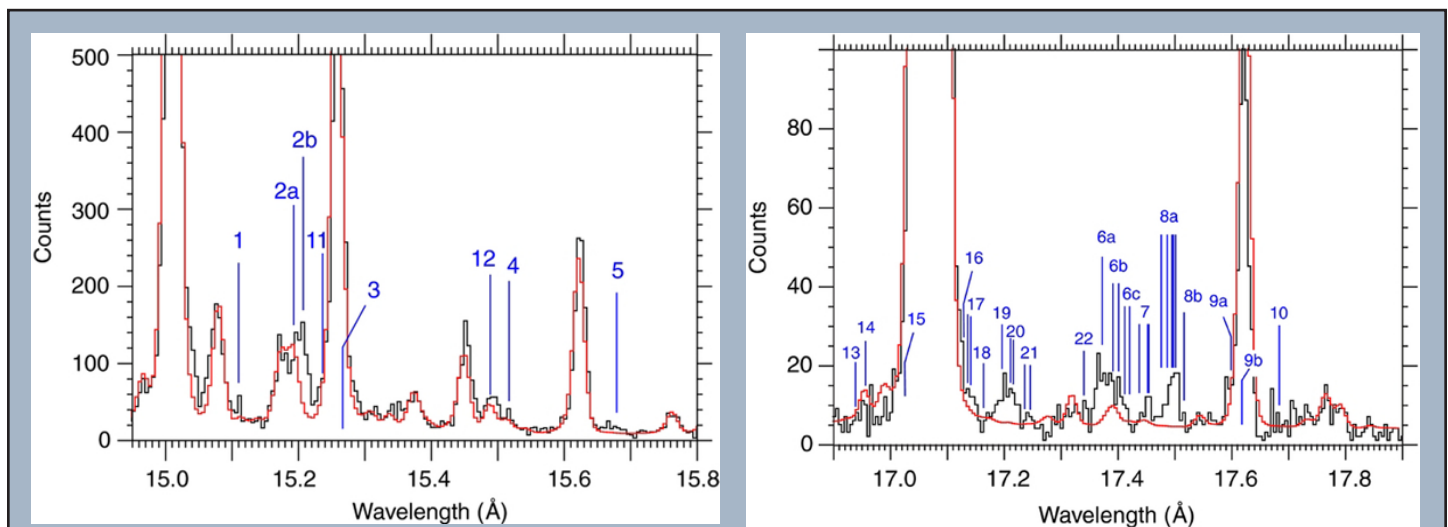

Fig. 1 - Capella HETG spectra with Fe XVI lines. The HETG data (black) are reasonably fit with an APEC model (red). However, some excess emission is seen and is very well explained by the newly-calculated locations of Fe XVI L-shell lines (numbered line identifications). (From Beiersdorfer et al. 2012.)

hole's orbital motion imprinted on them. As a "proof of concept" they have analyzed HETG observations of the binary GRO J1655-40, which consists of a ~5 M$_\odot$ black hole in a 2.6 day orbit with a ~2 M$_\odot$ companion star. Their analysis of dozens of narrow absorption lines includes a wind velocity for each line as well as the amplitude of the black hole's orbital motion, determined to be 90 km s^{-1} (Figure 3). Given the limited orbital coverage of the current data, it is certainly intriguing to see what data at other phases would show.

References

[1]Beiersdorfer, P., Diaz, F., Ishikawa, Y. 2012, ApJ 745, 167.

[2]CXC Ciao (4.5) `tg_findzo ahelp`: http://cxc.harvard.edu/ciao/ahelp/tg_findzo.html

[3]Hussain, G. A. J., Bickhouse, N. S., Dupree, A. K., Reale, F., Favata, F., and Jardine, M. M. 2012, MNRAS 423, 493.

[4]Marshall, H.L. 2012, Proc. of the SPIE, Vol. 8443 (arXiv:1211.0017).

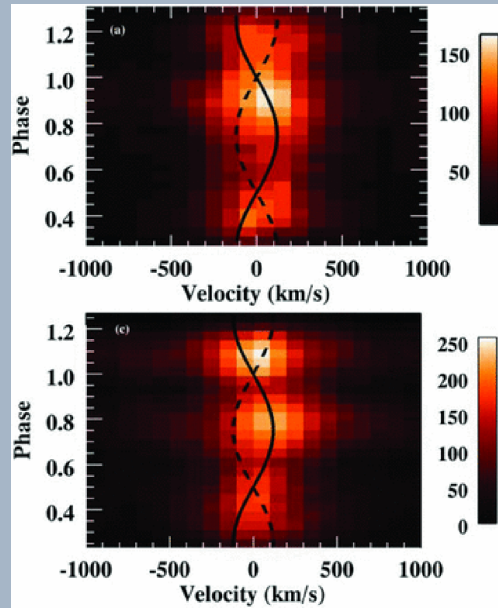[5]Zhang, S. N., Liao, J., Yao, Y. 2012, MNRAS 421, 3550.

Fig. 2 - Doppler images of the M dwarf binary, YY Gem. Two HETG observations each spanning a complete orbit are shown with time increasing from the bottom to top, in units of the orbital phase of the system. A given horizontal row shows the observed composite velocity profile at that time. The superposed sine curves indicate the velocities of the primary (black) and secondary (dashed). The emission is dominated by three flares, seen centered near phase 0.9 in the top image and phases 0.8 and 1.1 in the bottom. The velocity profiles suggest that two of these flares (top at 0.9 and bottom at 0.8) were associated with the primary star. (From Hussain et al. 2012.)
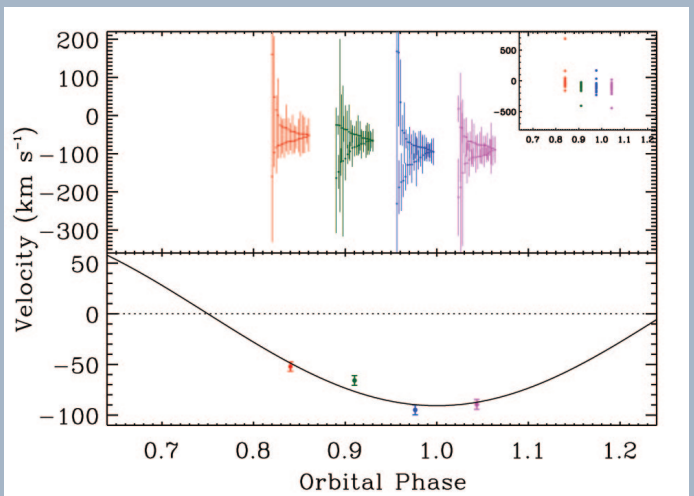

Fig. 3 - Inferred orbital velocity versus orbital phase of the black-hole binary GRO J1655-40. The top panel shows the 39 individual line measurements at each of the 4 phases. The bottom panel shows the weighted average of these velocities and the best-fit orbital velocity curve (black). (From Zhang et al. 2012.)